Joonhee M. An, Marco Califano, Alberto Franceschetti, and Alex Zunger

---

Excited-state relaxation in PbSe quantum dots

Joonhee M. An,[1] Marco Califano,[2] Alberto Franceschetti,[1,a)] and Alex Zunger[1,b)]

[1]*National Renewable Energy Laboratory, Golden, Colorado 80401, USA*
[2]*Institute of Microwaves and Photonics, School of Electronic and Electrical Engineering,*
University of Leeds, Leeds LS2 9JT, United Kingdom

In solids the phonon-assisted, nonradiative decay from high-energy electronic excited states to low-energy electronic excited states is picosecond fast. It was hoped that electron and hole relaxation could be slowed down in quantum dots, due to the unavailability of phonons energy matched to the large energy-level spacings ("phonon-bottleneck"). However, excited-state relaxation was observed to be rather fast (≤ 1 ps) in InP, CdSe, and ZnO dots, and explained by an efficient Auger mechanism, whereby the excess energy of electrons is nonradiatively transferred to holes, which can then rapidly decay by phonon emission, by virtue of the densely spaced valence-band levels. The recent emergence of PbSe as a novel quantum-dot material has rekindled the hope for a slow down of excited-state relaxation because hole relaxation was deemed to be ineffective on account of the widely spaced hole levels. The assumption of sparse hole energy levels in PbSe was based on an effective-mass argument based on the light effective mass of the hole. Surprisingly, fast intraband relaxation times of 1–7 ps were observed in PbSe quantum dots and have been considered contradictory with the Auger cooling mechanism because of the assumed sparsity of the hole energy levels. Our pseudopotential calculations, however, do not support the scenario of sparse hole levels in PbSe: Because of the existence of three valence-band maxima in the bulk PbSe band structure, hole energy levels are densely spaced, in contradiction with simple effective-mass models. The remaining question is whether the Auger decay channel is sufficiently fast to account for the fast intraband relaxation. Using the atomistic pseudopotential wave functions of $Pb_{2046}Se_{2117}$ and $Pb_{260}Se_{249}$ quantum dots, we explicitly calculated the electron-hole Coulomb integrals and the $P \rightarrow S$ electron Auger relaxation rate. We find that the Auger mechanism can explain the experimentally observed $P \rightarrow S$ intraband decay time scale without the need to invoke any exotic relaxation mechanisms. © *2008 American Institute of Physics*. [DOI: 10.1063/1.2901022]

INTRODUCTION

In insulating solids[1] and in large molecules,[2] optical excitation at energy Δ_{excess} above the first excited state leads to rapid, phonon-assisted intraband relaxation of the photoexcited electron and hole. As a result, photoluminescence is observed only from the lowest-energy excited state, irrespective of the magnitude of Δ_{excess} [Fig. 1(a)]. The emergence of semiconductor quantum dots has raised the hope that intraband carrier relaxation could be significantly slowed down via a "phonon-bottleneck" mechanism [Fig. 1(b)], in which phonon-assisted intraband transitions are inhibited by the large energy spacing between electronic levels. The existence of long-lived excited states could be beneficial to devices that utilize the excess energy Δ_{excess}. Examples include the expected extension of *radiative* intraband emission far into the mid-IR,[3] or the utilization of the excess energy Δ_{excess} to create additional electron-hole pairs.[4] This phonon-bottleneck scenario[5,6] was postulated on the basis that quantum confinement in zero-dimensional nanostructures increases the spacing between electronic energy levels, while

leaving the phonon energies largely unchanged. Indeed, in CdSe (Ref. 7) and PbSe (Refs. 8–10) nanocrystals, the spacings between the first and second electron levels [S and P in Fig. 1(a)] are 200–400 meV and 100–300 meV, respectively, far exceeding the LO phonon energies of ~30 (Ref. 11) and 17 meV,[3,11,12] respectively. Even in a much larger, self-assembled InGaAs/GaAs dots, the spacing between the electronic levels (~50 meV) is larger than the LO phonon energy (~30 meV).[13–16] When the spacing between electronic levels exceeds the phonon energy, one would expect[5,6] phonon-assisted relaxations to be slow, on account of the unavailability of energy-conserving phonons.[17] This scenario led to the expectation[4,5] of slow carrier relaxation in quantum dots [Fig. 1(b)].

However, fast, subpicosecond-to-picosecond excited-state relaxation times were observed in CdSe (Refs. 7 and 18–21), InP (Ref. 22), and ZnO (Ref. 22) quantum dots. Even in the much larger self-assembled InGaAs/GaAs dots, the observed[23] relaxation time was as fast as ~10 ps. This "first crisis" created by the experimental absence[7,18–22] of the theoretically expected[4,5] phonon bottleneck was addressed by suggesting that the phonon bottleneck for electrons is circumvented by fast electron-hole Auger scattering.[24] Whereas the spacing between electron levels is usually large in quan-

a)Electronic mail: alberto_franceschetti@nrel.gov.
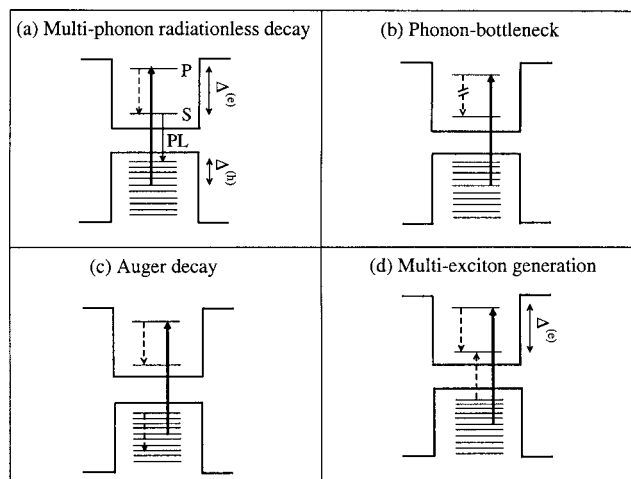b)Electronic mail: alex_zunger@nrel.gov.

FIG. 1. Electron relaxation mechanisms in quantum dots following optical excitation (bold upward arrow). (a) Multiphonon decay, where the *P*-to-*S* radiationless transition (dashed arrow) is phonon-assisted. (b) Phonon bottleneck, where the *P*-to-*S* transition is impeded by the absence of energy-conserving phonons. (c) Auger decay, where the *P*-to-*S* transition occurs by transfer of the electron excess energy to the hole. (d) Multiexciton generation, where the excited electron transfers its excess energy by creating an additional electron-hole pair.

tum dots, the spacing between hole levels can be rather small [10 meV in CdSe (Ref. 25) and InGaAs (Ref. 13) quantum dots]. Thus, the radiationless decay of excited electron states can be fast, provided that the excess energy of the electron can be efficiently transferred to the hole [Fig. 1(c)].[24] The question is whether the electron-hole Auger coupling in quantum dots is large enough to explain the observed ultrafast $P \rightarrow S$ electron relaxation time. This possibility was quantitatively examined by calculating the magnitude of the Auger coupling from pseudopotential theory.[25] It was found that for CdSe dots this hole-mediated electronic $P \rightarrow S$ decay time matched experiment[7,18–21] very well, both in magnitude and in its dependence on quantum-dot size. The same was true in self-assembled InGaAs/GaAs dots, where the calculated Auger lifetime[13] explained the observed $P \rightarrow S$ decay when both electrons and holes are present in the dot.

The Auger mechanism obviously requires the presence of a hole to be effective [Fig. 1(c)]. This mechanism as an explanation of the observed *P*-to-*S* electron relaxation was challenged by Guyot-Sionnest *et al.*,[26] who reported relatively fast (10–30 ps) electron decay in CdSe dots passivated by alkylamines or dodecanethiol ligands, which act as hole traps and thus separate the photogenerated hole from the electron. This slowing down of the *P*-to-*S* electron relaxation time by a factor of 2–5 (with respect to the case where electrons and holes are both present in the core of the dot) was interpreted as evidence for the need for another mechanism to explain electron relaxation, at least in the case where the hole is trapped at the surface of the dot. However, this qualitative expectation was not supported by a quantitative estimate of how much slowing down of the *P*-to-*S* relaxation is expected *under the Auger picture* for a given degree of hole localization. Such a quantitative calculation was recently provided by Califano,[27] who found that in CdSe nanocrystals efficient energy transfer can be achieved between a dot-

interior electron and a surface-trapped hole, leading to *P*-to-*S* electron relaxation rates in quantitative agreement with the experiment and consistent with the Auger interpretation of electron relaxation. Thus, the alternative mechanisms, while possible, are not forced upon us by any conflict of simpler mechanisms with experimental data.

The emergence of PbSe as a novel colloidal-dot material[3,12,28–31] has rekindled the hope for a slowdown of excited-state relaxation because PbSe was deemed to be a very different material than the previously studied CdSe, InP, and ZnO quantum dots. Indeed, the hole effective masses of PbSe (longitudinal mass $m_l = 0.07$, transverse mass $m_t = 0.034$)[11] are light. In a simple, infinite-barrier particle-in-a-box or $k \cdot p$ model,[32] this would imply large spacings between the hole levels, thus impeding fast hole relaxation and therefore impeding effective Auger relaxation of electrons. It was further suggested[29,30] that a slow excited-state relaxation would explain the observation of multiexciton generation in PbSe [Fig. 1(d)], a process that competes with the Auger relaxation channel [Figs. 1(a)–1(c)].

Contrary to expectations[28,30,32] that the excited-state decay in PbSe quantum dots would be slow, Wehrenberger *et al.*[3] first showed that the decay is actually faster than the experimental temporal resolution of 4 ps. Subsequent refined measurements by Schaller *et al.*[12] revealed a low-temperature decay time of only ∼1.6 ps for 19 Å radius dots and ∼2.7 ps for 35 Å radius dots, not much slower than CdSe. These observations were followed by the measurements of Harbold *et al.*,[28] who measured a room-temperature decay time of 3.5–6.5 ps for nanocrystal size $R = 20$–30 Å. Recently, Bonati *et al.*[33] reported upconversion photoluminescence measurements of excited-state relaxation rates in PbSe nanocrystals. They found relaxation times ranging from 0.85 to 1.3 ps for PbSe nanocrystals 1.7 to 3.6 nm in radius, the relaxation time being the largest for the smallest nanocrystals. Furthermore, multiexciton generation [Fig. 1(d)], which was initially thought to be particular to PbSe dots, was later observed in several other materials [CdSe (Ref. 34), PbS (Ref. 30), and PbTe (Ref. 35)], for which the hole level spacing is not known to be particularly large. This "second crisis," created by the experimental absence[3,12,28] of the theoretically expected[28–30,32] slow excited-state relaxation in PbSe quantum dots, led to the statement that "this is not understood, and there is a need for a novel mechanism to explain these results."[3] Indeed, rather exotic mechanisms, involving very strong acoustic coupling,[3] or multiphonon emission triggered by nonadiabatic electron-hole interaction,[12] were suggested to explain the fast $P \rightarrow S$ decay in PbSe dots.

Examination of the literature cited above reveals that this second crisis was created by the commonly held opinion that excited-state relaxation in PbSe must be slow on account of the widely spaced hole levels. In turn, the expectation of widely spaced hole levels was based on effective-mass-like models[12,30,32] that describe quantum dot states on the basis of very few bulk crystal band-edge states. A close examination[9] of the band structure of bulk PbSe[36] reveals, however, that there are a few valence-band extrema near the valence-band maximum (VBM), originating from different valleys

(L, Σ, etc.) in the Brillouin zone. Thus, dot hole states could evolve from a number of host crystal valleys, an effect that is not describable by single-valley effective mass models[12,30,32] and that was recently confirmed by optical absorption measurements.[37] Indeed, atomistic multivalley, multiband pseudopotential calculations[9] have shown that the hole states in PbSe dots are rather closely spaced (by a few meV), in sharp contrast to the expectations of simple models.[12,30,32] The significant density of hole states of PbSe places this material in a similar qualitative[38] class with other dot materials, and contradicts the expectation of a phonon bottleneck. Having established that the hole energy levels are sufficiently dense to allow for fast, phonon-assisted hole relaxation,[9] in this work, we examine the second prerequisite for fast electron relaxation, namely, the existence of an efficient Auger relaxation channel.

To examine the consequences of the electronic structure of PbSe quantum dots on the Auger decay rate, we have used the atomistically calculated energy levels and wave functions to compute the $P \rightarrow S$ Auger lifetime τ_A. We find $\tau_A = 0.1-0.2$ ps for $R = 15.3$ Å and $\tau_A = 6-16$ ps for $R = 30.6$ Å at room temperature (the range corresponding to different assumed broadening factors for the electronic energy levels). While these decay times are somewhat longer than the 0.12 and 0.25 ps observed in CdSe dots[39] of radius $R = 17$ and 23 Å, respectively, the differences do not appear to be qualitative. We conclude that there is no phonon bottleneck in PbSe quantum dots because of the closely spaced hole levels and efficient electron-hole Auger scattering [Fig. 1(c)]. The reason why multiexciton generation [Fig. 1(d)] is observed in PbSe is that this process is even faster[10] than the Auger process.

METHOD OF CALCULATION

When a high-energy electron-hole pair is created by photon absorption, it rapidly decays via phonon emission until it reaches the (e_p, h_s) configuration, where the electron occupies one of the quasidegenerate P-like conduction states $\{e_p\}$ and the hole occupies one of the S-like valence states $\{h_s\}$ [see Fig. 1(a)]. This fast phonon-assisted decay is enabled by the large density of hole and electron states.[9] When the electron reaches the e_p levels, however, it can no longer relax by phonon emission because of the large energy gap between the e_p levels and the e_s levels. Thus, the (e_p, h_s) configuration is dynamically "stable" with respect to phonon-assisted relaxation, and the Auger relaxation channel becomes the dominant decay channel.

The Auger relaxation rate is calculated here using time-dependent perturbation theory (Fermi's golden rule). The initial and final states of the Auger process are described by single Slater determinants. In a previous work on CdSe quantum dots,[25] we used a *limited* configuration-interaction (CI) expansion—where only coupling between different (e_p, h_s) configurations was included—to calculate the initial and final states of the Auger process. We found that such limited CI expansion leads only to minor changes in the Auger rate compared to a calculation based on single Slater determinants. Note that in a *full* CI description, where the excitons are coherent mixtures of all electron-hole pairs, the matrix elements between the initial and final states of the Auger process would be zero. The rationale for using a limited CI description is that the fast phonon decay channel introduces an efficient decoherence mechanism for the photogenerated excitons. In other words, we consider the case where the system has been "prepared" in the initial configuration (e_p, h_s) by fast phonon-assisted decay.

According to Fermi's golden rule, the Auger relaxation rate is given by

$$\tau_A^{-1}(h_s, e_p) = \frac{\Gamma}{\hbar} \sum_n \sum_s \frac{|J(h_s, e_p; h_n, e_s)|^2}{(\varepsilon_{e_p} - \varepsilon_{h_s} + \varepsilon_{h_n} - \varepsilon_{e_s})^2 + (\Gamma/2)^2}, \quad (1)$$

where the sum runs over the final hole states $\{h_n\}$ and electron states $\{e_s\}$, and Γ is a Lorentzian broadening that phenomenologically describes inhomogeneous line broadening due to size-distribution effects as well as homogeneous line broadening. The set of final configurations (h_n, e_s) in Eq. (1) includes 100 hole states h_n, as well as the eight quasidegenerate electron states e_s. The Auger matrix elements are given by Coulomb integrals of the form

$$J(i, j; k, l) = \sum_{\sigma_1, \sigma_2} \int \int \frac{\psi_i^*(\mathbf{r}_1, \sigma_1) \psi_j^*(\mathbf{r}_2, \sigma_2) \psi_k(\mathbf{r}_1, \sigma_1) \psi_l(\mathbf{r}_2, \sigma_2)}{\epsilon(\mathbf{r}_1, \mathbf{r}_2) |\mathbf{r}_1 - \mathbf{r}_2|} d\mathbf{r}_1 d\mathbf{r}_2, \quad (2)$$

where $\{\psi_i(\mathbf{r}, \sigma)\}$ are the single-particle wave functions (which depend on the spatial variable $\mathbf{r}$ and the spin variable σ) and $\epsilon(\mathbf{r}_1, \mathbf{r}_2)$ is the microscopic dielectric constant of the dot.

To generate the single-particle eigensolutions $\{\psi_i, \varepsilon_i\}$ needed to evaluate Eqs. (1) and (2), we solve the effective Schrödinger equation,

$$\left[-\tfrac{1}{2} \nabla^2 + V(\mathbf{r}) + V_{\text{SO}} \right] \psi_i(\mathbf{r}, \sigma) = \varepsilon_i \psi_i(\mathbf{r}, \sigma), \quad (3)$$

where the wave functions $\psi_i(\mathbf{r}, \sigma)$ are expanded in a plane wave basis set and V_{SO} is the spin-orbit operator. The local potential $V(\mathbf{r})$ is represented as a superposition of screened atomic pseudopotentials for atom species α at site $\mathbf{d}_\alpha$ in
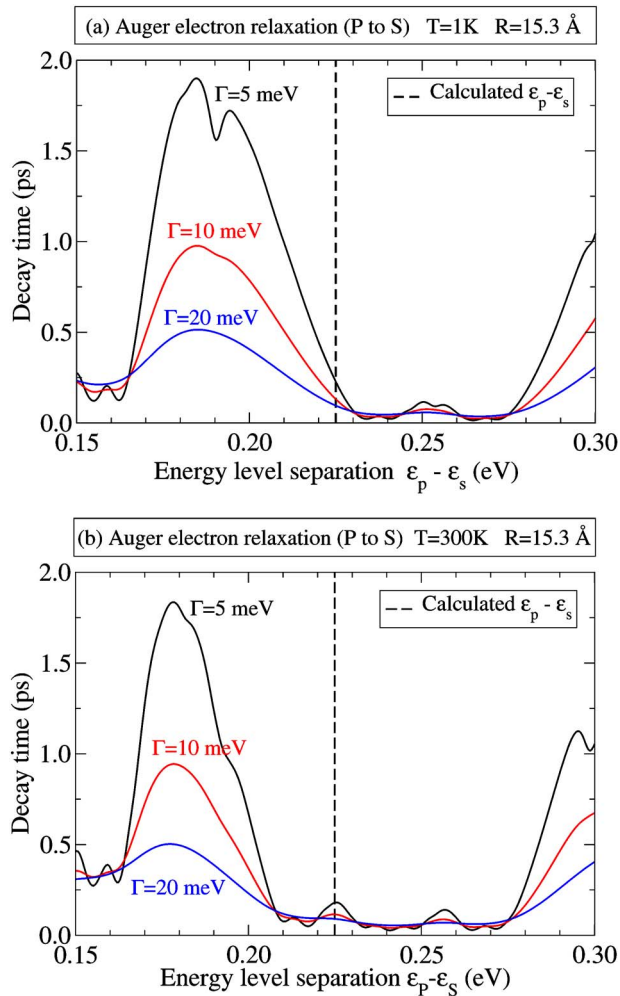
FIG. 2. (Color online) Calculated Auger electron relaxation time of the 15.3 Å radius PbSe dot at (a) $T=1$ K and (b) 300 K for three different Lorentzian broadenings Γ in Eq. (1), assuming the dot gap does not depend on T. The dotted vertical line indicates the pseudopotential calculated value of $\varepsilon_p - \varepsilon_s$.

cell $\mathbf{R}$,

$$V(\mathbf{r}) = \sum_\alpha \sum_{\mathbf{R}} v_\alpha(|\mathbf{r} - \mathbf{R} - \mathbf{d}_\alpha|). \tag{4}$$

A correct description of the single-particle energy levels of quantum dots requires a theoretical model that can accurately describe a few physical effects: (i) The existence of multiple band extrema in the corresponding *bulk* band structure. Previously published first-principles band-structure calculations of bulk PbSe (Ref. 36) show that a few valence-band extrema exist within ~ 0.5 eV of the VBM. All effective-mass-based methods applied to PbSe to date include but a single valence band valley, so they all miss this contribution to the hole density of states of PbSe quantum dots. (ii) The splitting of the L-valley band-edge states and their anisotropic effective masses. The only other atomistic (not effective mass) calculation of large PbSe quantum dots is the tight-binding calculation of Allan and Delerue.[40] Unfortunately, the particular tight-binding fit of Ref. 40 did not
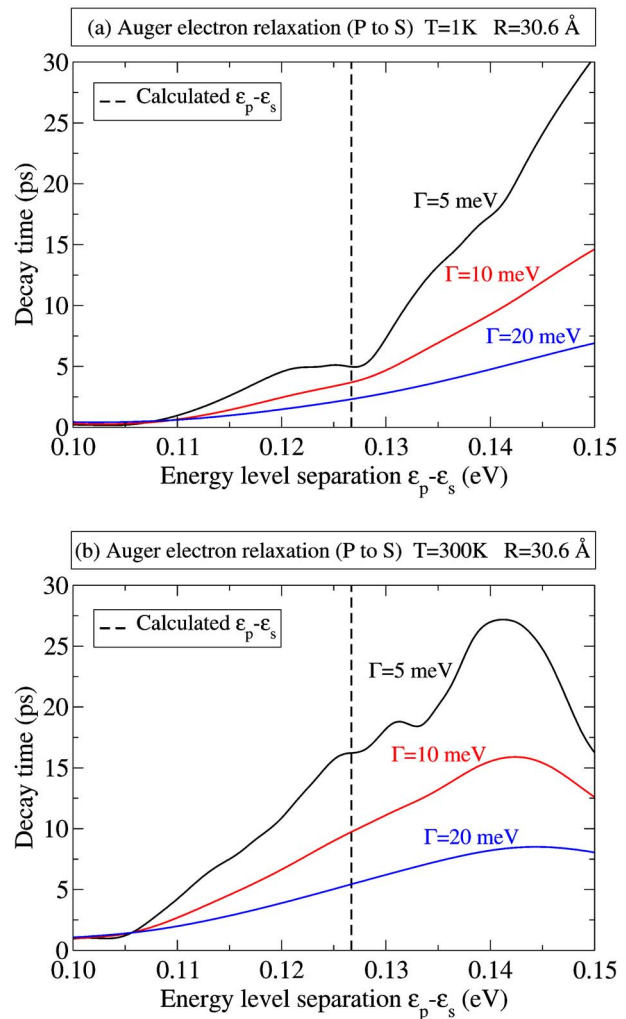

FIG. 3. (Color online) Same as in Fig. 1 but for the 30.6 Å radius PbSe dot.

correctly reproduce the effective-mass anisotropy of the L valleys.[9]

Here, we consider two quantum dots; $Pb_{260}Se_{249}$ ($R=15.3$ Å) and $Pb_{2046}Se_{2117}$ ($R=30.6$ Å). All surface dangling bonds were passivated by ligand potentials.[9,10] References 9 and 10 give the results of interband absorption spectra, intraband absorption spectra, and multiexciton generation of these dots. To evaluate Coulomb integrals of Eq. (2), we use a microscopic dielectric function of the form

$$\epsilon^{-1}(\mathbf{r}_1, \mathbf{r}_2) = \epsilon_{out}^{-1}(\mathbf{r}_1, \mathbf{r}_2) + [\epsilon_{in}^{-1}(\mathbf{r}_1, \mathbf{r}_2) - \epsilon_{out}^{-1}(\mathbf{r}_1, \mathbf{r}_2)]m(\mathbf{r}_1)m(\mathbf{r}_2), \tag{5}$$

where $m(\mathbf{r})$ is 1 for $|\mathbf{r}| \leq R-d$ (here, $d=1$ Å), decays to zero as $\sqrt{[\sin(\pi(R-|\mathbf{r}|)/2d)+1]/2}$ between $R-d$ and $R+d$, and remains zero for $|\mathbf{r}| \geq R+d$. The introduction of the mask function $m(\mathbf{r})$ is consistent with recent first-principles calculations by Cartoixà and Wang,[41] showing that the dielectric function inside a quantum dot is bulklike, whereas at the surface, it decays into the dielectric function of the material surrounding the dot. In the following, we use $\epsilon_{in}=22.9$ and $\epsilon_{out}=1$, corresponding to the macroscopic dielectric constants of bulk PbSe and vacuum, respectively.
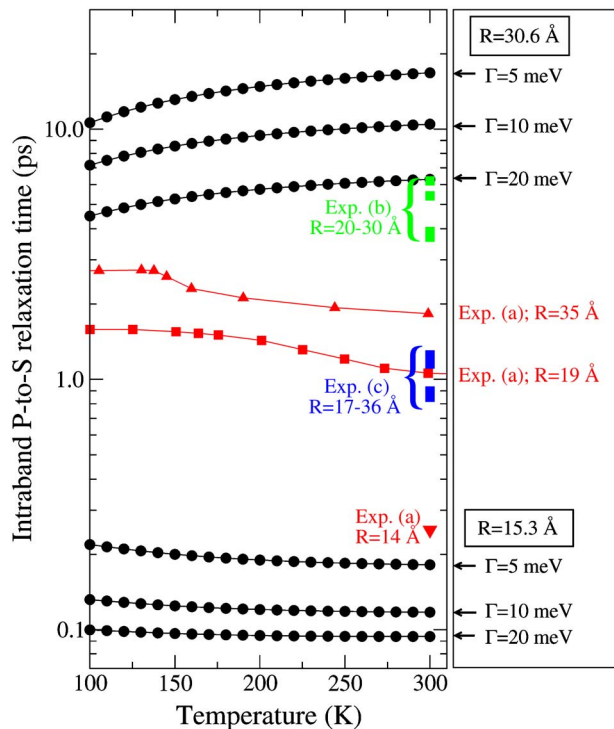
FIG. 4. (Color online) Calculated P-to-S Auger relaxation time $\tau_A(T)$ (solid circles) for PbSe dots of radius $R=15.6$ Å and $R=30.6$ Å, for three values of the broadening factor Γ in Eq. (1). Also shown are the measured exciton relaxation times as a function of temperature from Ref. 12 [Exp. (a)], and the room-temperature exciton relaxation times from Ref. 28 [Exp. (b)] and Ref. 33 [Exp. (c)].

Whereas the e_p-e_s energy separation is too large (≥ 130 meV, corresponding to $\sim 8\hbar\omega_{LO}$) to allow for efficient phonon-assisted electron relaxation, the energy splittings within the $\{e_p\}$ and $\{h_s\}$ manifolds are very small (a few meV in a 30.6 Å dot), so we assume that the $\{e_p\}$ and $\{h_s\}$ levels are thermally populated. The temperature dependence of the Auger decay rate is computed using the Boltzmann statistics,

$$\tau_A^{-1}(T) = \frac{\sum_\gamma \tau_\gamma^{-1} e^{-(E_\gamma-E_0)/K_BT}}{\sum_\gamma e^{-(E_\gamma-E_0)/K_BT}}, \qquad (6)$$

where the sum runs over the 64 exciton configurations γ (of energy E_γ and intrinsic Auger lifetime τ_γ), in which the electron occupies one of the eight lowest-energy e_p conduction states and the hole occupies one of the eight highest-energy h_s valence states. E_0 is the lowest-energy such configuration. The method of Eqs. (1)–(6) has been previously used[25] for calculating Auger relaxation rate and recombination rate in CdSe dots, where it produced a close agreement with the experiment. Here, we note that bulk PbSe has a strong and anomalous band gap temperature dependence,[11] presumably due to strong electron-phonon coupling, whereas our calculation is done for a static lattice, neglecting electron-phonon coupling and assuming a temperature-independent level spacing.

AUGER RELAXATION TIME

Figures 2 and 3 show our calculated $P \to S$ Auger relaxation time τ_A at two different temperatures, $T=1$ and 300 K, and for two different dot sizes, $R=15.3$ Å and $R=30.6$ Å. In Figs. 2 and 3, we plot τ_A as a function of the value of the S-P splitting $\varepsilon_p-\varepsilon_s$. This is accomplished by adding a term Δ_{sp} to the first term in the denominator of Eq. (1). The case $\Delta_{sp}=0$ corresponds to the calculated pseudopotential value of the S-P splitting $\varepsilon_p-\varepsilon_s$ (vertical dashed lines in Figs. 2 and 3). The variation of τ_A with the value of Δ_{sp} demonstrates the extent to which energy conservation influences the Auger rate. The oscillations of τ_A correlate with the presence of hole states h_n in and out of resonance with the value of the $\varepsilon_p-\varepsilon_s$ energy. The room-temperature calculated values of τ_A for $\Delta_{sp}=0$ are 0.18, 0.11, and 0.09 ps for $\Gamma=5$, 10, and 20 meV, respectively, in the case of the $R=15.3$ Å dot, and 16.2, 9.7, and 5.4 ps for the 30.6 Å dot. Harbold et al.[28,31] reported photoluminescence linewidths of the order of 100 meV in PbSe nanocrystals. We find, however, that the value of τ_A does not significantly change when Γ increases above 20 meV.

Figure 4 shows $\tau_A(T)$ of the 15.3 and the 30.6 Å PbSe quantum dots as a function of temperature for three different values of the broadening factor Γ (5, 10, and 20 meV). We find that the Auger relaxation time $\tau_A(T)$ of the $R=30.6$ Å dot increases with increasing temperature, while $\tau_A(T)$ of the $R=15.3$ Å dot decreases slightly with temperature. For example, for $\Gamma=10$ meV, $\tau_A(T)$ increases from 7.1 ps at 100 K to 10.4 ps at 300 K in the case of the $R=30.6$ Å dot, while it decreases from 0.13 to 0.12 ps for the 15.3 Å dot. Also shown in Fig. 4 are the measured values of the exciton relaxation times.[12,28,33] Since experiments measure the relaxation time from an excited state (e.g., P_h-P_e) to the exciton ground state (S_h-S_e), the experimental data is not directly comparable with our calculations of the $P \to S$ electron relaxation rate because the exciton relaxation time is affected by the hole relaxation. Nevertheless, Schaller et al.[12] reported complementary dynamics for the $1P$ and $1S$ exciton populations, suggesting that hole relaxation may not be the rate limiting factor in PbSe quantum dots. The calculated values of $\tau_A(T)$ are in qualitative agreement with the measured values,[12,28,33] although our calculations for the $R=30.6$ Å dot do not reproduce the observed slope with temperature,[12] presumably because we assume a static lattice, neglecting electron-phonon coupling.

To understand the origin of the calculated temperature dependence of $\tau_A(T)$ (Fig. 4), we show in Fig. 5 the calculated intrinsic Auger lifetimes τ_γ of the 64 initial exciton states, originating from the eight lowest-energy P-like electron states and the eight highest-energy S-like hole states. Also shown in Fig. 5 (lower panels) are the Boltzmann weights $e^{-(E_\gamma-E_0)/K_BT}$ of the 64 exciton states at $T=300$ K. We see that in the case of the $R=30.6$ Å dot [Fig. 5(b)] the intrinsic Auger lifetimes τ_γ tend to increase with the exciton energy E_γ. As a result, the Auger lifetime $\tau_A(T)$ increases with temperature (Fig. 4). In the case of the $R=15.3$ Å dot [Fig. 5(a)], the intrinsic Auger lifetimes τ_γ have a nonmono-
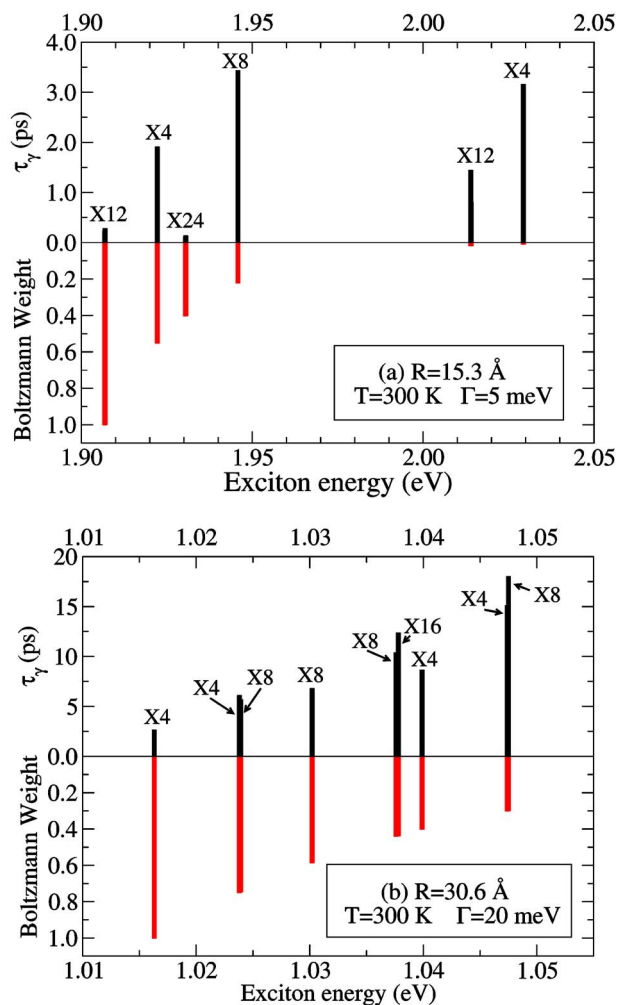
FIG. 5. (Color online) Calculated intrinsic Auger lifetimes τ_γ [darker (black) vertical bars] for (a) 15.3 Å radius and (b) 30.6 Å radius PbSe quantum dots as a function of the exciton energy E_γ. Also shown are the Boltzmann factors at $T=300$ K [lighter (red) vertical bars].

tonic dependence on the exciton energy E_γ, so the thermal-averaged Auger lifetime τ_A depends more weakly on temperature.

SUMMARY

The observed fast $P \rightarrow S$ intraband relaxation times[3,12,28] of 1–7 ps for PbSe dots of radius ranging from 20 to 35 Å have been previously considered to be contradictory with the light hole and electron effective masses of PbSe and the presumed mirrorlike symmetry between conduction and valence energy levels. Our pseudopotential calculations[9,10] refuted the presumption of mirrorlike symmetry: Because of the existence of three valence-band maxima in the bulk PbSe band structure, hole energy levels are more densely spaced than electron energy levels, thereby opening up Auger scattering as a possible source of the fast $P \rightarrow S$ intraband relaxation. We find that the Auger mechanism can explain the experimentally observed intraband $P \rightarrow S$ relaxation time scale without the need to invoke any exotic relaxation mechanisms. However, inclusion of the temperature dependence of the electron and hole spacings may be needed to obtain a closer agreement between the calculated temperature depen-

dence of τ_A and experiment. The existence of efficient multiexciton generation in PbSe (Refs. 29 and 30) and in other quantum-dot materials (Refs. 30, 34, and 35) does not conflict with the existence of picosecond fast excited-state Auger relaxation, because multiexciton generation is considerably faster.[10]

[1] C. H. Henry and D. V. Lang, IEEE Trans. Electron Devices **21**, 745 (1974).
[2] R. Englman and J. Jortner, Mol. Phys. **18**, 145 (1970).
[3] B. L. Wehrenberg, C. Wang, and P. Guyot-Sionnest, J. Phys. Chem. B **106**, 10634 (2002).
[4] A. Nozik, Physica E (Amsterdam) **14**, 115 (2002).
[5] U. Bockelmann and G. Bastard, Phys. Rev. B **42**, 8947 (1990).
[6] H. Benisty, C. M. Sotomayor-Torrès, and C. Weisbuch, Phys. Rev. B **44**, 10945 (1991).
[7] V. I. Klimov, D. W. McBranch, C. A. Leatherdale, and M. G. Bawendi, Phys. Rev. B **60**, 13740 (1999).
[8] P. Liljeroth, P. A. Z. van Emmichoven, S. G. Hickey, H. Weller, B. Grandidier, G. Allan, and D. Vanmaekelbergh, Phys. Rev. Lett. **95**, 086801 (2005).
[9] J. M. An, A. Franceschetti, S. V. Dudiy, and A. Zunger, Nano Lett. **6**, 2728 (2006).
[10] A. Franceschetti, J. M. An, and A. Zunger, Nano Lett. **6**, 2191 (2006).
[11] Landolt-Bornstein, Group III Condensed Matter (Springer-Verlag, Berlin, 1998), Vol. 41.
[12] R. D. Schaller, J. M. Pietryga, S. V. Goupalov, M. A. Petruska, S. A. Ivanov, and V. I. Klimov, Phys. Rev. Lett. **95**, 196401 (2005).
[13] G. A. Narvaez, G. Bester, and A. Zunger, Phys. Rev. B **74**, 075403 (2006).
[14] S. Hameau, Y. Guldner, O. Verzelen, R. Ferreira, and G. Bastard, Phys. Rev. Lett. **83**, 4152 (1999).
[15] V. M. Fomin, V. Gladilin, J. Devreese, E. Pokatilov, S. N. Balaban, and S. Klimin, Solid State Commun. **105**, 113 (1998).
[16] V. M. Fomin, E. P. Pokatilov, J. T. Devreese, S. N. Klimin, V. N. Gladilin, and S. N. Balaban, Solid-State Electron. **42**, 1309 (1998).
[17] If strong electron-lattice coupling exists, the adiabatic approximation breaks down, leading to no phonon bottleneck, even if there is some energetic mismatch. See Refs. 14–16.
[18] V. I. Klimov and D. W. McBranch, Phys. Rev. Lett. **80**, 4028 (1998).
[19] P. Guyot-Sionnest, M. Shim, C. Matranga, and M. Hines, Phys. Rev. B **60**, R2181 (1999).
[20] C. Burda, S. Link, M. Mohamed, and M. El-Sayed, J. Phys. Chem. B **105**, 12 286 (2001).
[21] U. Woggon, H. Giessen, F. Gindele, O. Wind, B. Fluegel, and N. Peyghambarian, Phys. Rev. B **54**, 17681 (1996).
[22] M. Shim and P. Guyot-Sionnest, Phys. Rev. B **64**, 245342 (2001).
[23] T. S. Sosnowski, T. B. Norris, H. Jiang, J. Singh, K. Kamath, and P. Bhattacharya, Phys. Rev. B **57**, R9423 (1998); T. Müller, F. F. Schrey, G. Strasser, and K. Unterrainer, Appl. Phys. Lett. **83**, 3572 (2003); M. De Giorgi, C. Lingk, G. von Plessen, J. Feldmann, S. De Rinaldis, A. Passaseo, M. De Vittorio, R. Cingolani, and M. Lomascolo, *ibid.* **79**, 3968 (2001); T. F. Boggess, L. Zhang, D. G. Deppe, D. L. Huffaker, and C. Cao, *ibid.* **78**, 276 (2001).
[24] A. L. Efros, V. A. Kharchenko, and M. Rosen, Solid State Commun. **93**, 281 (1995).
[25] L.-W. Wang, M. Califano, A. Zunger, and A. Franceschetti, Phys. Rev. Lett. **91**, 056404 (2003).
[26] P. Guyot-Sionnest, B. Wehrenberg, and D. Yu, J. Chem. Phys. **123**, 074709 (2005).
[27] M. Califano (in press).
[28] J. M. Harbold, H. Du, T. D. Krauss, K.-S. Cho, C. B. Murray, and F. W. Wise, Phys. Rev. B **72**, 195312 (2005).
[29] R. D. Schaller and V. I. Klimov, Phys. Rev. Lett. **92**, 186601 (2004).

[30] R. J. Ellingson, M. C. Beard, J. C. Johnson, P. Yu, O. I. Micic, A. J. Nozik, A. Shabaev, and A. L. Efros, Nano Lett. **5**, 865 (2005).

[31] J. M. Harbold and F. W. Wise, Phys. Rev. B **76**, 125304 (2007).

[32] I. Kang and F. W. Wise, J. Opt. Soc. Am. B **14**, 1632 (1997).

[33] C. Bonati, A. Cannizzo, D. Tonti, A. Tortschanoff, F. van Mourik, and M. Chergui, Phys. Rev. B **76**, 033304 (2007).

[34] R. D. Schaller, M. A. Petruska, and V. I. Klimov, Appl. Phys. Lett. **87**, 253102 (2005).

[35] J. E. Murphy, M. C. Beard, A. G. Norman, S. P. Ahrenkiel, J. C. Johnson, P. Yu, O. I. Micic, R. J. Ellingson, and A. J. Nozik, J. Am. Chem. Soc. **128**, 3241 (2006).

[36] S. H. Wei and A. Zunger, Phys. Rev. B **55**, 13605 (1997).

[37] R. Koole, G. Allan, C. Delerue, A. Meijerink, D. Vanmaekelbergh, and A. Houtepen, Small **4**, 127 (2008).

[38] PbSe does have different properties relative to ordinary II-VI materials, e.g., its dielectric constant is 22.9, while the dielectric constant of CdSe is 6.3. However, this leads to only quantitative differences in carrier decay, not qualitative differences.

[39] V. Klimov, J. Phys. Chem. B **104**, 6112 (2000).

[40] G. Allan and C. Delerue, Phys. Rev. B **70**, 245321 (2004).

[41] X. Cartoixà and L.-W. Wang, Phys. Rev. Lett. **94**, 236804 (2005).